PHYSICAL REVIEW C **83**, 031301(R) (2011)

Improved nuclear matter calculations from chiral low-momentum interactions

K. Hebeler,[1,2] S. K. Bogner,[3] R. J. Furnstahl,[2] A. Nogga,[4] and A. Schwenk[5,6]

[1]*TRIUMF, 4004 Wesbrook Mall, Vancouver, British Columbia, Canada V6T 2A3*

[2]*Department of Physics, The Ohio State University, Columbus, Ohio 43210, USA*

[3]*National Superconducting Cyclotron Laboratory and Department of Physics and Astronomy, Michigan State University, East Lansing, Michigan 48844, USA*

[4]*Institute for Advanced Simulations, Institut für Kernphysik and Jülich Centre for Hadron Physics, Forschungszentrum Jülich, D-52425 Jülich, Germany*

[5]*ExtreMe Matter Institute EMMI, GSI Helmholtzzentrum für Schwerionenforschung GmbH, D-64291 Darmstadt, Germany*

[6]*Institut für Kernphysik, Technische Universität Darmstadt, D-64289 Darmstadt, Germany*

(Received 17 December 2010; published 7 March 2011)

We present nuclear matter calculations based on low-momentum interactions derived from chiral effective field theory potentials. The current calculations use an improved treatment of the three-nucleon force (3NF) contribution that includes a corrected combinatorial factor beyond Hartree-Fock that was omitted in previous nuclear matter calculations. We find realistic saturation properties using parameters fit only to few-body data, but with larger uncertainty estimates from cutoff dependence and the 3NF parametrization than in previous calculations.

DOI: 10.1103/PhysRevC.83.031301 PACS number(s): 21.65.−f, 21.30.−x, 21.60.Jz, 21.10.Dr

Major advances in nuclear structure theory over the past decade have been made by expanding the reach of few-body calculations that use microscopic interactions between nucleons. This progress has unambiguously established the quantitative role of three-nucleon forces (3NF) for the ground state and spectra of light nuclei ($A \leqslant 12$) [1,2]. Pioneering extensions to larger nuclei reveal new facets of the 3NF, such as its role in determining the location of the neutron dripline [3,4] and in elucidating the doubly magic nature of ^{48}Ca [5]. Pushing these successes to still heavier nuclei, which includes most of the table of nuclides, is a fundamental challenge for low-energy nuclear physics.

The historical route to heavy nuclei is through infinite nuclear matter, a theoretical uniform limit that first turns off the Coulomb interaction, which otherwise drives heavier stable nuclei toward an imbalance of neutrons over protons and eventually, instability. However, predicting nuclear matter based on microscopic internucleon forces has proved to be an elusive target. In particular, few-body fits have not sufficiently constrained 3NF contributions around saturation density such that nuclear matter calculations are predictive. Nuclear matter saturation is very delicate, with the binding energy resulting from cancellations of much larger potential and kinetic energy contributions. When a quantitative reproduction of empirical saturation properties was obtained, it was imposed by hand through the adjustment of short-range three-body forces (see, for example, Refs. [6,7]).

The lack of progress toward controlled nuclear matter calculations has long been hindered by the difficulty of the nuclear many-body problem when conventional nuclear potentials are used. The present calculations continue an alternative approach to nuclear matter using soft Hamiltonians derived from interactions fit only to few-body ($A \leqslant 4$) data. We find realistic saturation properties within our theoretical uncertainty bounds without adjustment of parameters. This progress follows by applying several recent developments: systematic starting Hamiltonians based on chiral effective field theory (EFT) [8], renormalization group (RG) methods [9] to soften the short-range repulsion and short-range tensor components of the initial chiral interactions so that convergence of many-body calculations is vastly accelerated [10–12], and a new 3NF fitting procedure to the ^{4}He radius rather than the binding energy [2]. (Alternative expansions using chiral interactions are described in Refs. [8,13,14]). The calculations here also employ an improved treatment of the 3NF contribution in many-body perturbation theory compared to Refs. [10,15], which includes the full treatment of 3NF double-exchange diagrams and corrected 3NF combinatorial factors beyond Hartree-Fock. Note that previous calculations of neutron matter [16,17] and finite nuclei [3,5] are not affected.

Our results are summarized in Fig. 1, which shows the energy per particle of symmetric matter as a function of Fermi momentum k_F, or the density $\rho = 2k_F^3/(3\pi^2)$. A gray square representing the empirical saturation point is shown in each of the nuclear matter figures. Its boundaries reflect the ranges of nuclear matter saturation properties predicted by phenomenological Skyrme energy functionals that most accurately reproduce properties of finite nuclei [18]. Although this determination cannot be completely model independent, the value is generally accepted for benchmarking infinite matter. In the future, calculations of the properties of finite nuclei will allow one to compare directly to experimental data.

The calculations of Fig. 1 start from the N^{3}LO nucleon-nucleon (NN) potential (EM 500 MeV) of Ref. [19]. This NN potential is RG-evolved to low-momentum interactions $V_{\mathrm{low}\,k}$ with a smooth $n_{\mathrm{exp}} = 4$ regulator [20]. For each cutoff Λ, two couplings that determine the shorter-range parts of the N^{2}LO 3NF [21] are fit to the ^{3}H binding energy and the ^{4}He matter radius using exact Faddeev and Faddeev-Yakubovsky methods

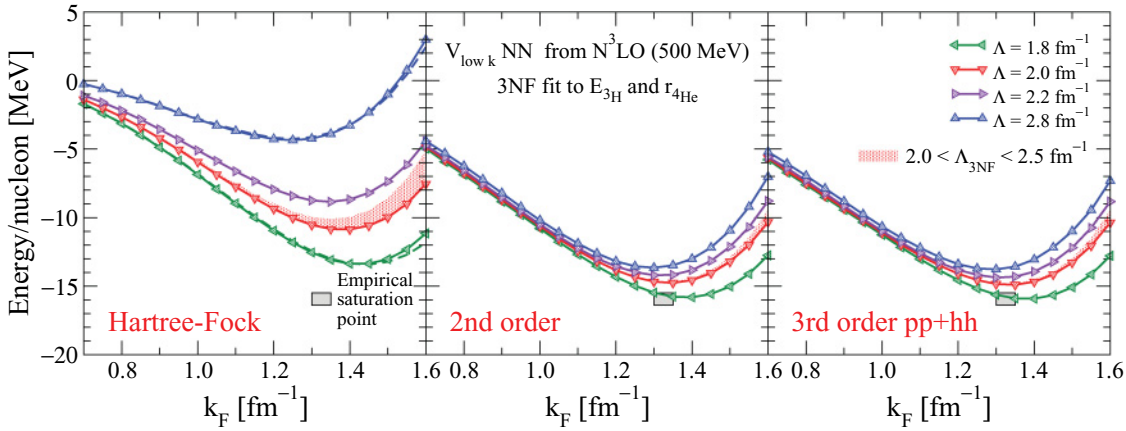

FIG. 1. (Color online) Nuclear matter energy per particle versus Fermi momentum k_F at the Hartree-Fock level (left) and including second-order (middle) and third-order particle-particle/hole-hole contributions (right), based on evolved N^{3}LO NN potentials and 3NF fit to $E_{^3\mathrm{H}}$ and $r_{^4\mathrm{He}}$. Theoretical uncertainties are estimated by the NN (lines)/3N (band) cutoff variations.

as in Ref. [22]. Our 3NF central fit values are given in Table I; we estimate that c_D has an uncertainty of approximately 0.4 due to the uncertainties of the charge radius in ^{4}He. We use a 3NF regulator of the form $\exp\{-[(p^2 + 3/4q^2)/\Lambda_{3\mathrm{NF}}^2]^{n_{\mathrm{exp}}}\}$ with $n_{\mathrm{exp}} = 4$, where the 3N cutoff $\Lambda_{3\mathrm{NF}}$ is allowed to vary independently of the NN cutoff, which probes the sensitivity to short-range three-body physics. The shaded regions in Fig. 1 show the range of results for 2.0 fm^{-1} $< \Lambda_{3\mathrm{NF}} <$ 2.5 fm^{-1} at fixed $\Lambda = 2.0$ fm^{-1}.

Nuclear matter is calculated in three approximations: Hartree-Fock (left), Hartree-Fock plus second-order contributions (middle), and additionally summing third-order particle-particle and hole-hole contributions (right). The technical details regarding the treatment of the 3NF and the many-body calculation are as for neutron matter in Ref. [16]. We first construct a density-dependent two-body interaction from the 3NF by summing one particle over occupied states in the Fermi sea (see also Ref. [23]). This conversion simplifies the many-body calculation significantly and allows the inclusion of all 3NF double-exchange terms beyond Hartree-Fock, which were only approximated in Refs. [10,15]. Furthermore, we have corrected the combinatorial factors at the normal-ordered two-body level of the 3NF from 1/6 to 1/2 in diagrams beyond Hartree-Fock used in these references (see Refs. [9,16] for detailed discussions of these factors, which are correctly included in Refs. [3,5,16,17]). To our knowledge, previous calculations in the literature of nuclear matter using normal-ordered 3NF contributions need the same correction.

TABLE I. Results for the c_D and c_E couplings fit to $E_{^3\mathrm{H}} = -8.482$ MeV and to the point charge radius $r_{^4\mathrm{He}} = 1.464$ fm (based on Ref. [26]) for the NN/3N cutoffs and different EM/EGM/PWA c_i values used. For $V_{\mathrm{low}\,k}$ (SRG) interactions, the 3NF fits lead to $E_{^4\mathrm{He}} = -28.22\ldots-28.45$ MeV ($-28.53\ldots-28.71$ MeV).

	$V_{\mathrm{low}\,k}$		SRG	
Λ or $\lambda/\Lambda_{3\mathrm{NF}}$ (fm)	c_D	c_E	c_D	c_E
1.8/2.0 (EM c_i's)	+1.621	−0.143	+1.264	−0.120
2.0/2.0 (EM c_i's)	+1.705	−0.109	+1.271	−0.131
2.0/2.5 (EM c_i's)	+0.230	−0.538	−0.292	−0.592
2.2/2.0 (EM c_i's)	+1.575	−0.102	+1.214	−0.137
2.8/2.0 (EM c_i's)	+1.463	−0.029	+1.278	−0.078
2.0/2.0 (EGM c_i's)	−4.381	−1.126	−4.828	−1.152
2.0/2.0 (PWA c_i's)	−2.632	−0.677	−3.007	−0.686

The dashed lines in the left panel of Fig. 1 (for $\Lambda =$ 1.8 and 2.8 MeV) show the exact Hartree-Fock energy in comparison with the results obtained using the effective two-body interaction (solid lines). The excellent agreement supports the use of this density-dependent two-body approximation for symmetric nuclear matter. For the results beyond the Hartree-Fock level we use full momentum-dependent single-particle Hartree-Fock propagators. We have checked that the energies obtained using a self-consistent second-order spectrum overlap with the band of curves in Fig. 1.

The Hartree-Fock results show that nuclear matter is bound even at this simplest level. A calculation without approximations should be independent of the cutoffs, so the spread in Fig. 1 sets the scale for omitted many-body contributions. The second-order results show a significant narrowing of this spread over a large density region. It is encouraging that our results agree with the empirical saturation point within the uncertainty in the many-body calculation and omitted higher-order many-body forces implied by the cutoff variation (the greater spread compared to Ref. [15] is mostly attributable to the corrected combinatorial factor). We stress that the cutoff dependence of order 3 MeV around saturation density is small compared to the total size of the kinetic energy ($\approx$23 MeV) and potential energy (≈ -38 MeV) at this density. Moreover, the cutoff dependence is smaller at $k_F \approx 1.1$ fm^{-1}, which more resembles the typical densities in medium-mass to heavy nuclei ($\rho = 0.11$ fm^{-3}). For all cases in the right panel of Fig. 1, the compressibility $K =$ 175–210 MeV is in the empirical range.

The inclusion of third-order contributions gives only small changes from second order except at the lowest densities shown. This is consistent with nuclear matter being

perturbative for low-momentum interactions, at least in the particle-particle channel [10]. The difference at small densities is not surprising: the presence of a two-body bound state necessitates a nonperturbative summation in the dilute limit. We note that below saturation density, the ground state is not a uniform system, but breaks into clusters (see, for example, Ref. [24]).

In chiral EFT without explicit deltas, 3N interactions start at N^{2}LO [21] and their contributions are given diagrammatically by

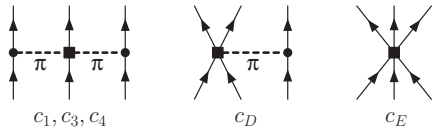

We assume that the c_i coefficients of the long-range two-pion-exchange part are not modified by the RG. At present, we rely on the N^{2}LO 3NF as a truncated "basis" for low-momentum 3N interactions and determine the c_D and c_E couplings by a fit to data for all cutoffs [22]. In the future, fully evolved three- and four-body forces in momentum space starting from chiral EFT will be available (see Ref. [25] for an application of evolved 3NF in a harmonic-oscillator basis). The fit values of Table I are natural and the predicted ^{4}He binding energies are very reasonable. We have also verified that the resulting 3NF becomes perturbative in $A = 3, 4$ (see also Refs. [10,15,22]), i.e., the calculated individual 3NF contributions are largely unchanged if evaluated for wave functions using NN forces only.

The evolution of the cutoff Λ to smaller values is accompanied by a shift of physics. In particular, effects due to iterated tensor interactions are replaced by three-body contributions. The role of the 3NF for saturation is demonstrated in Fig. 2. The two pairs of curves show the difference between the nuclear matter results for NN-only and NN plus 3N interactions. It is evident that saturation is driven by the 3NF [10,15]. Even for $\Lambda = 2.8$ fm^{-1}, which is similar to the lower cutoffs in chiral EFT potentials, saturation is at too high a density without the 3NF. Nevertheless, as in previous results [10,15], the 3N contributions and the c_D, c_E fits are natural, and the same is expected for the ratio of three- to four-body contributions.

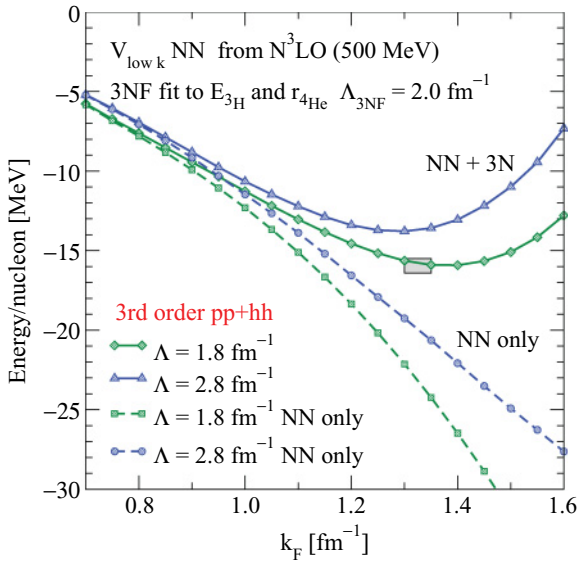

FIG. 2. (Color online) Nuclear matter energy of Fig. 1 at the third-order level compared to NN-only results for two representative NN cutoffs and a fixed 3N cutoff.

The smooth RG evolution used in the results so far is not the only choice for low-momentum interactions. A recent development is the use of flow equations to evolve Hamiltonians, which we refer to as the similarity renormalization group (SRG) [27–29]. The flow parameter λ, which has dimensions of a momentum, is a measure of the degree of decoupling in momentum space. Few-body results for roughly the same value of SRG λ and smooth $V_{low\,k}$ Λ have been remarkably similar (see, for example, Ref. [11]). With either RG method, we can also change the initial interaction. The results presented so far all start from a chiral EFT potential at a single order with one choice of EFT regulator implementation and values. There are several alternatives available [8,19,30], which are almost phase-shift equivalent (but the χ^2 is not equally good up to $E_{lab} \approx 300$ MeV). Universality for phase-shift equivalent chiral EFT potentials as Λ decreases was shown for smooth-cutoff $V_{low\,k}$ interactions in Refs. [9,20] in the form of the collapse of different initial potentials to the same matrix elements in each partial wave channel. An analogous collapse has been found for N^{3}LO potentials evolved by the SRG to smaller λ [9].

Based on this universal collapse for low-momentum interaction matrix elements, it is natural to expect a similar collapse for the energy per particle in nuclear matter. We consider four different chiral NN potentials: the N^{3}LO potential by Entem and Machleidt [19] for two different cutoffs 500 and 600 MeV, and the N^{3}LO NN potential by Epelbaum *et al.* [30] (EGM) for two different cutoff combinations 550/600 MeV and 600/700 MeV. The results for the energy are presented in Fig. 3. The upper panel shows the energies for $V_{low\,k}$ NN-only interactions derived from different chiral NN potentials (solid lines) in comparison to Brueckner-Hartree-Fock (BHF) (which means resummed particle-particle ladder) results based on unevolved chiral potentials (dashed lines). For clarity, we only display the two extreme BHF results. As shown in the lower panel we find a model dependence of about 13 MeV for the unevolved N^{3}LO potentials around saturation density and approximately 2 MeV for the $V_{low\,k}$ and SRG low-momentum interactions, comparable to the cutoff variation in Fig. 1. The latter spread reflects the residual RG/SRG dependence on the initial interactions.

By supplementing the low-momentum NN interactions with corresponding 3NFs we can probe the sensitivity of the energy to uncertainties in the c_i coefficients (see also Refs. [16,31,32]). We consider three different cases: first, we take low-momentum interactions evolved from the N^{3}LO NN potential EM 500 MeV (EM c_i's: $c_1 = -0.81$ GeV^{-1}, $c_3 = -3.2$ GeV^{-1}, $c_4 = 5.4$ GeV^{-1}); second, low-momentum interactions from the EGM 550/600 MeV potential (EGM c_i's: $c_1 = -0.81$ GeV^{-1}, $c_3 = -3.4$ GeV^{-1}, $c_4 = 3.4$ GeV^{-1}); and third, low-momentum interactions from the EM 500 MeV potential combined with the central c_i values obtained from the NN partial wave analysis [33] (PWA c_i's:

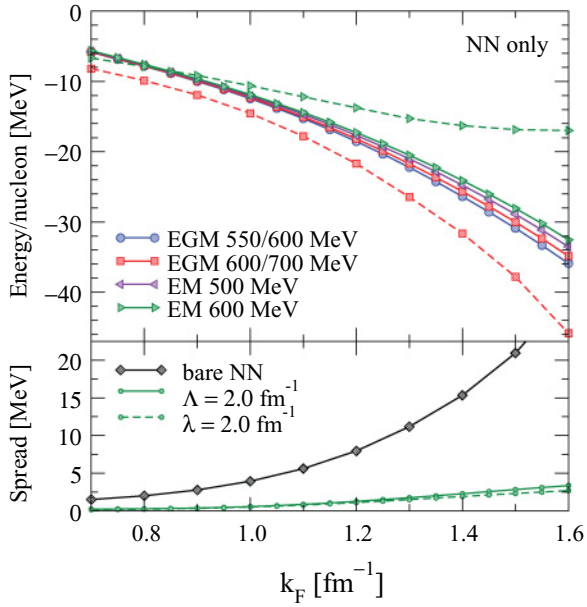

FIG. 3. (Color online) Nuclear matter NN-only results for different chiral N^{3}LO potentials (EM [19] and EGM [30]). The upper panel shows the third-order results for $V_{\mathrm{low}\,k}$-evolved interactions at $\Lambda = 2.0$ fm^{-1} (solid lines) and Brueckner-Hartree-Fock results for the two unevolved chiral potentials that provide the lowest and highest energies (dashed lines), EGM 600/700 MeV and EM 600 MeV. The lower panel shows the maximal spread of the energy results at these two cutoff scales Λ for $V_{\mathrm{low}\,k}$ and λ for SRG-evolved NN interactions.

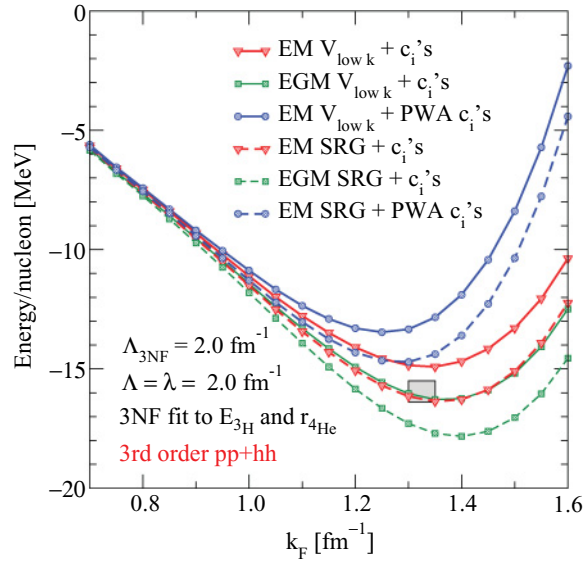

FIG. 4. (Color online) Nuclear matter energy at the third-order level comparing low-momentum $V_{\mathrm{low}\,k}$ with SRG-evolved chiral NN interactions for 3NF with different EM/PWA/EGM c_i values used (see text).

$c_1 = -0.76$ GeV^{-1}, $c_3 = -4.78$ GeV^{-1}, $c_4 = 3.96$ GeV^{-1}). The fit values for c_D and c_E are given in Table I.

The resulting nuclear matter energies are shown in Fig. 4. For all three cases we find realistic saturation properties within the theoretical uncertainties implied by the cutoff dependence shown in Fig. 1 and the NN interaction dependence shown in Fig. 3. The difference between $V_{\mathrm{low}\,k}$ and SRG results for a given set of c_i is similar to the NN-only case (see Fig. 1), which helps support the general nature of the 3NF fit. However, the present sensitivity study can clearly only provide a first estimate for the energy spread due to uncertainties of the c_i couplings. A more systematic study will require a correlation analysis based on a larger set of results.

The theoretical errors of our nuclear matter results arise from truncations in the initial chiral EFT Hamiltonian, the approximation of the 3NF, and the many-body approximations. Corrections to the present calculation include higher-order many-body terms, in particular, particle-hole corrections, and contributions from higher-order many-body forces and from 3NF contributions that cannot be expressed in terms of density-dependent two-body interactions. While the improvements in the cutoff dependence suggest that these corrections are relatively small, an approach such as coupled cluster theory that can perform a high-level resummation is ultimately necessary for a robust validation.

While nuclear matter has lost to light nuclei its status as the first step to nuclear structure, it is still key as a step to heavier nuclei and astrophysical applications like the structure of neutron stars [17]. Our results can help with efforts to develop *ab initio* density functional theory (DFT) based on expanding about nuclear matter [34]. This is analogous to the application of DFT in quantum chemistry and condensed matter starting with the uniform electron gas in local-density approximations and adding constrained derivative corrections. Phenomenological energy functionals (such as Skyrme) for nuclei have impressive successes but lack a (quantitative) microscopic foundation based on nuclear forces and seem to have reached the limits of improvement with the current form of functionals [35,36]. At present, the theoretical errors of our results, while small on the scale of the potential energy per particle, are too large to be quantitatively competitive with existing functionals. The implementation of higher-order chiral Hamiltonians and their RG evolution can be expected to provide more accurate and reliable predictions. However, there is also the possibility of fine tuning to heavy nuclei, of using EFT/RG to guide next-generation functional forms [37,38], and of benchmarking with *ab initio* methods for low-momentum interactions. Work in these directions is in progress.

In summary, we have presented new results for nuclear matter based on chiral NN and 3N interactions with RG evolution. The chiral EFT framework provides a systematic improvable Hamiltonian while the softening of nuclear forces by RG evolution enhances the convergence and control of the many-body calculation. The empirical saturation point is reproduced within our estimates of uncertainties despite input only from few-body data. Because of the fine cancellations, however, significant reduction of these uncertainties will be needed before direct DFT calculations of nuclei are competitive. Nevertheless, these results are very promising for a unified description of all nuclei and nuclear matter.

We thank J. W. Holt for helpful discussions. This work was supported in part by NSERC, the NSF under Grants No. PHY-0653312, No. PHY-0758125, and No. PHY-1002478,

the UNEDF SciDAC Collaboration under DOE Grant No. DE-FC02-07ER41457, the Helmholtz Alliance Program of the Helmholtz Association, Contract No. HA216/EMMI "Extremes of Density and Temperature: Cosmic Matter in the Laboratory," and the DFG through Grant No. SFB 634. TRIUMF receives funding via a contribution through the NRC Canada. Part of the numerical calculations were performed at the JSC, Jülich, Germany.

[1] S. C. Pieper, R. B. Wiringa, and J. Carlson, Phys. Rev. C **70**, 054325 (2004); S. C. Pieper, Riv. Nuovo Cimento **031**, 709 (2008).
[2] P. Navrátil, V. G. Gueorguiev, J. P. Vary, W. E. Ormand, and A. Nogga, Phys. Rev. Lett. **99**, 042501 (2007); P. Navrátil, S. Quaglioni, I. Stetcu, and B. R. Barrett, J. Phys. G **36**, 083101 (2009).
[3] T. Otsuka, T. Suzuki, J. D. Holt, A. Schwenk, and Y. Akaishi, Phys. Rev. Lett. **105**, 032501 (2010).
[4] G. Hagen, T. Papenbrock, D. J. Dean, M. Hjorth-Jensen, and B. Velamur Asokan, Phys. Rev. C **80**, 021306 (2009).
[5] J. D. Holt, T. Otsuka, A. Schwenk, and T. Suzuki, arXiv:1009.5984.
[6] A. Akmal, V. R. Pandharipande, and D. G. Ravenhall, Phys. Rev. C **58**, 1804 (1998).
[7] A. Lejeune, U. Lombardo, and W. Zuo, Phys. Lett. B **477**, 45 (2000).
[8] E. Epelbaum, H.-W. Hammer, and U.-G. Meißner, Rev. Mod. Phys. **81**, 1773 (2009).
[9] S. K. Bogner, R. J. Furnstahl, and A. Schwenk, Prog. Part. Nucl. Phys. **65**, 94 (2010).
[10] S. K. Bogner, A. Schwenk, R. J. Furnstahl, and A. Nogga, Nucl. Phys. A **763**, 59 (2005).
[11] S. K. Bogner, R. J. Furnstahl, P. Maris, R. J. Perry, A. Schwenk, and J. P. Vary, Nucl. Phys. A **801**, 21 (2008).
[12] S. Bacca, A. Schwenk, G. Hagen, and T. Papenbrock, Eur. Phys. J. A **42**, 553 (2009).
[13] N. Kaiser, S. Fritsch, and W. Weise, Nucl. Phys. A **697**, 255 (2002).
[14] A. Lacour, J. A. Oller, and U.-G. Meißner, Ann. Phys. **326**, 241 (2011).
[15] S. K. Bogner, R. J. Furnstahl, A. Nogga, and A. Schwenk, arXiv:0903.3366.
[16] K. Hebeler and A. Schwenk, Phys. Rev. C **82**, 014314 (2010).
[17] K. Hebeler, J. M. Lattimer, C. J. Pethick, and A. Schwenk, Phys. Rev. Lett. **105**, 161102 (2010).
[18] M. Bender, P.-H. Heenen, and P.-G. Reinhard, Rev. Mod. Phys. **75**, 121 (2003).
[19] D. R. Entem and R. Machleidt, Phys. Rev. C **68**, 041001(R) (2003).
[20] S. K. Bogner, R. J. Furnstahl, S. Ramanan, and A. Schwenk, Nucl. Phys. A **784**, 79 (2007); K. Hebeler, A. Schwenk, and B. Friman, Phys. Lett. B **648**, 176 (2007).
[21] U. van Kolck, Phys. Rev. C **49**, 2932 (1994); E. Epelbaum, A. Nogga, W. Glöckle, H. Kamada, U.-G. Meißner, and H. Witala, *ibid.* **66**, 064001 (2002).
[22] A. Nogga, S. K. Bogner, and A. Schwenk, Phys. Rev. C **70**, 061002(R) (2004).
[23] J. W. Holt, N. Kaiser, and W. Weise, Phys. Rev. C **81**, 024002 (2010).
[24] C. J. Horowitz and A. Schwenk, Nucl. Phys. A **776**, 55 (2006).
[25] S. K. Bogner, R. J. Furnstahl, and R. J. Perry, Ann. Phys. **323**, 1478 (2008); E. D. Jurgenson, P. Navratil, and R. J. Furnstahl, Phys. Rev. Lett. **103**, 082501 (2009).
[26] I. Sick, Phys. Rev. C **77**, 041302 (2008).
[27] S. D. Glazek and K. G. Wilson, Phys. Rev. D **48**, 5863 (1993); F. Wegner, Ann. Phys. (Leipzig) **3**, 77 (1994).
[28] S. K. Bogner, R. J. Furnstahl, and R. J. Perry, Phys. Rev. C **75**, 061001(R) (2007).
[29] An alternative non-RG use of unitary transformations to reduce correlations in many-body wave functions is described in R. Roth, H. Hergert, P. Papakonstantinou, T. Neff, and H. Feldmeier, Phys. Rev. C **72**, 034002 (2005), and references therein.
[30] E. Epelbaum, W. Glöckle, and U.-G. Meißner, Nucl. Phys. A **747**, 362 (2005).
[31] L. Tolos, B. Friman, and A. Schwenk, Nucl. Phys. A **806**, 105 (2008).
[32] V. Bernard, Prog. Part. Nucl. Phys. **60**, 82 (2008).
[33] M. C. M. Rentmeester, R. G. E. Timmermans, and J. J. de Swart, Phys. Rev. C **67**, 044001 (2003).
[34] S. K. Bogner, R. J. Furnstahl, and L. Platter, Eur. Phys. J. A **39**, 219 (2009); B. Gebremariam, T. Duguet, and S. K. Bogner, Phys. Rev. C **82**, 014305 (2010).
[35] G. F. Bertsch, B. Sabbey, and M. Uusnakki, Phys. Rev. C **71**, 054311 (2005).
[36] M. Kortelainen, J. Dobaczewski, K. Mizuyama, and J. Toivanen, Phys. Rev. C **77**, 064307 (2008).
[37] B. Gebremariam, S. K. Bogner, and T. Duguet, Nucl. Phys. A **851**, 17 (2011).
[38] M. Stoitsov, M. Kortelainen, S. K. Bogner, T. Duguet, R. J. Furnstahl, B. Gebremariam, and N. Schunck, Phys. Rev. C **82**, 054307 (2010).